Building Simulation 2005

Ninth International IBPSA Conference
Montréal, Canada
August 15-18, 2005

EVALUATING TURBULENCE MODELS FOR 3-D FLOWS IN ENCLOSURE BY TOPOLOGY

Lars Køllgaard Voigt
ANSYS Europe Ltd.
West Central 127, Milton Park
Abingdon, Oxfordshire OX14 4SA
United Kingdom
Email: Lars.Voigt@ansys.com

ABSTRACT

Computational Fluid Dynamics (CFD) has evolved from an academic tool to an important commercial design tool over the past decades. In the present paper the accuracy of two equation turbulence models for 3-D internal air flows is investigated in terms of mean quantities and topological aspects. Results for pseudo 2-D and full 3-D simulations using the k-ε model and the Baseline (BSL) k-ω model of Menter, respectively, are compared with LDA measurements (Nielsen, 1990) and PIV measurements (Pedersen & Meyer, 2002). In order to explain similarities and differences between simulation and experiments, a topological apparatus is outlined. The main conclusion of this work is that the BSL k-ω model of Menter is superior to the k-ε model when flow structures are to be predicted.

INTRODUCTION

The scope of Computational Fluid Dynamics (CFD) has developed from academic to highly commercial during the past four decades. With the increased use of CFD for commercial purposes, the development of practical guidelines has turned out to be an important issue. Practical guidelines for HVAC applications typically involve suggestions for the choice of turbulence model, choice of boundary conditions, grid dependency studies, grid refinement near walls, convergence criterion and difference scheme (CFX,2004), the ERCOFTAC Guidelines, (Sørensen & Nielsen, 2003). In the author's opinion these guidelines are important and should be addressed when publishing papers on CFD. However, it is remarkably that none of the practical guidelines addresses a qualitative measure such as the flow pattern. The flow pattern must be assumed to be extremely important, when predicting for example distribution of particles and chemical reactions.

It can be difficult to set up qualitative measures of the flow pattern. In many practical setups this may not be possible at all. Nevertheless, the theory from non-linear differential equations (Grimshaw, 1990) can provide such a measure for certain geometries. It is one of the main objectives of this paper to demonstrate how the theory from non-linear differential equations can provide a qualitative measure of the accuracy of a CFD simulation. Moreover, the results indicate that the choice of turbulence model for internal flows is not a straightforward matter, and therefore this issue should be considered carefully.

The test case considered is the Annex 20 room (Nielsen, 1990). The flow in this room contains both regions of fully turbulent and purely laminar flow, which is representative for the flows in ventilated spaces (Davidson et al, 2000). Moreover, both Laser Doppler Anemometer (LDA) measurements (Nielsen, 1990) and Particle Image Velocimetry (PIV) measurements (Pedersen & Meyer, 2002), exist for this geometry. Previous investigations showed that 2-D simulations can never reproduce the experimental 3-D flow pattern (Voigt, 2002). Moreover, it was found that a k-ω turbulence model provided better results than a k-ε model, when the location of critical points was to be predicted. In the present paper the simulations (Voigt, 2002) are extended to three dimensions, leading to the appearance of three dimensional flow topologies.

The paper is organised as follows: First the test case is presented. Then the topological apparatus is outlined followed by a short description of the numerics with special emphasis on the turbulence models. Then the computational results for pseudo 2-D and full 3-D simulations are discussed and finally the conclusions are drawn.

TESTCASE

The test case employed in this study is the well known Annex 20 test case (Nielsen, 1990). The test case with dimensions is shown in figure 1.

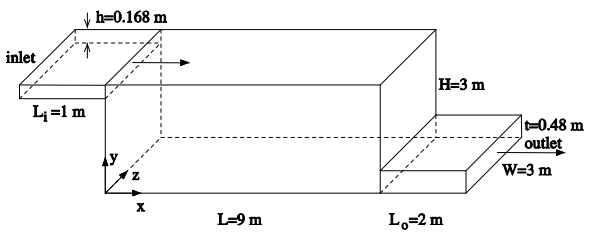

Figure 1: The isothermal Annex 20 test case

The test case is isothermal and air is supplied at the inlet with a velocity of 0.455 *m/s* in order to ensure Re=5000 based on the inlet height. From experiments (Nielsen, 1990) the turbulence intensity in the inlet is specified to be 4 %, and the length scale is chosen to be h/10=0.0168 *m* (Voigt, 2001).

TOPOLOGY

Topology can be a valuable tool when a qualitative description of the flow is desired. As mentioned in the introduction this will be important when considering particle movement, since these can be strongly influenced by the flow pattern. Previously, a discussion of the topologies relevant for two dimensional flow simulations and PIV experiments has been presented (Voigt *et al*, 2003). Below the results will briefly be summarized.

In this work, topology is interpreted as a systematic tool that provides a full qualitative description of the flow (Voigt *et al*, 2003). The approach involves two steps: First the critical points are located and then the critical points are classified in accordance with theory from non-linear differential equations (Grimshaw, 1990).

In two-dimensional flows the types of critical points that can occur are restricted by the Hamiltonian property of the stream function. Thus, the only non-degenerate possibilities for critical points are centres and saddles. The orbits near such critical points are shown in figure 2.

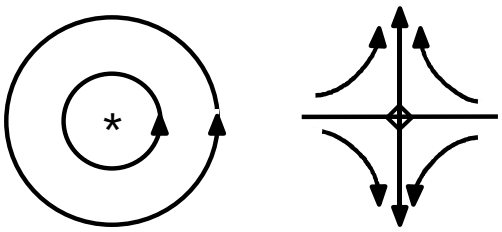

Figure 2: The orbits close to a centre point (left), and a saddle point (right).

For the saddle points it has been suggested to distinguish between attachment points and separation points (Hartnack, 1999). The flow pattern near an attachment point and a separation point is shown in figure 3.

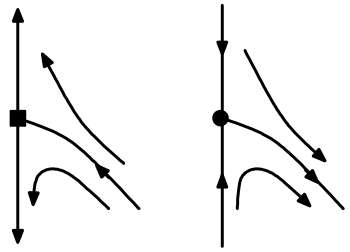

Figure 3: Attachment point located on a vertical wall (left). Separation point located on a vertical wall (right).

When three dimensional flows are considered, several types of critical points can exist. For example a spiral point can replace a centre if the flow is not exactly two-dimensional. The spiral can be either stable or unstable, see the orbits in figure 4.

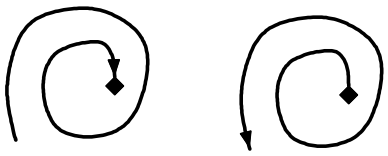

Figure 4: The orbits close to a stable spiral point (left) and an unstable spiral point (right)

This concludes the presentation of the topological apparatus. Only the types of critical points found in the experiments and simulations presented in this work has been described. However, several other types of critical points exist (Grimshaw, 1990)

NUMERICS

Turbulence models

The governing equations are continuity and the Navier-Stokes equations. The equations are time-averaged, and the set of equations are closed using a two equation turbulence model. Since two different turbulence models were employed and the choice of turbulence model had a significant impact on the flow, the tested models are discussed briefly in the following.

For the time-averaged equations, the purpose of the turbulence model is to model the Reynolds stresses. On the assumption that there exist an analogy between viscous stresses and Reynolds stresses, the task can be reduced to modelling the eddy viscosity appearing in the Boussinesq approximation. A relative simple way of modelling the eddy viscosity is to model the spatial variation of this quantity by a transport equation. More sophisticated models can be employed by expressing the eddy viscosity in terms of turbulent kinetic energy, k, and dissipation of turbulent kinetic energy, ε. The relation between the eddy viscosity, k and ε is found from dimensional

analysis, and transport equations are derived for *k* and ε, respectively. These types of models are referred to as the two-equation turbulence models and they are the most widely used for engineering applications. For this reason it was chosen to focus on these models in the present study. The models employed were the k-ε model and the Baseline (BSL) k-ω model (Menter, 1994)

For the k-ε model the eddy viscosity is given by

$$\mu_t = C_\mu \rho \frac{k^2}{\varepsilon} \tag{1}$$

This introduces the new variables k and ε, into the system of equations. The new variables are modelled by two transport equations, which take the form

$$\frac{\partial(\rho k)}{\partial t} + \frac{\partial \rho U_j k}{\partial x_j} = \frac{\partial}{\partial x_j}\left[\left(\mu + \frac{\mu_t}{\sigma_k}\right)\frac{\partial k}{\partial x_j}\right] + P_k - \rho\varepsilon \tag{2}$$

and

$$\frac{\partial(\rho\varepsilon)}{\partial t} + \frac{\partial \rho U_j \varepsilon}{\partial x_j} = \frac{\partial}{\partial x_j}\left[\left(\mu + \frac{\mu_t}{\sigma_\varepsilon}\right)\frac{\partial \varepsilon}{\partial x_j}\right] + \frac{\varepsilon}{k}(C_{\varepsilon 1} P_k - C_{\varepsilon 2}\rho\varepsilon) \tag{3}$$

A problem which occurs when using the k-ε model is that the friction velocity will depend on the distance to the first grid point. This problem can be circumvented by employing scalable wall functions in which a limiter is applied to the dimensionless near wall distance. The limiting value is typically set to 11.06, which is the intersection point between the logarithmic layer and linear near wall profile (CFX, 2004)

For the k-ω models the eddy viscosity is given by

$$\mu_t = \rho \frac{k}{\omega} \tag{4}$$

This introduces the variables k and ω into the system of equations. The BSL k-ω based model blends the k-ε model and the k-ω model. For this models the transport equations for *k* and ω take the form

$$\frac{\partial(\rho k)}{\partial t} + \frac{\partial \rho U_j k}{\partial x_j} = \frac{\partial}{\partial x_j}\left[\left(\mu + \frac{\mu_t}{\sigma_{k3}}\right)\frac{\partial k}{\partial x_j}\right] + P_k - \beta'\rho k\omega \tag{5}$$

and

$$\frac{\partial(\rho\omega)}{\partial t} + \frac{\partial \rho U_j \omega}{\partial x_j} = \frac{\partial}{\partial x_j}\left[\left(\mu + \frac{\mu_t}{\sigma_{\omega 3}}\right)\frac{\partial \omega}{\partial x_j}\right] + (1-F_1)2\rho\frac{1}{\sigma_{\omega 2}\omega}\frac{\partial k}{\partial x_j}\frac{\partial \omega}{\partial x_j} + \alpha_3\frac{\omega}{k}P_k - \beta_3\rho\omega^2 \tag{6}$$

The blending function F_1 is designed to be one close to surfaces, corresponding to a k-ω model, and zero away from surfaces, corresponding to a k-ε model.

The boundary layer is handled using an automatic near-wall switch. This implies that first grid point is not treated as being outside the viscous sub layer, but is virtually moved down through the viscous sub layer when the mesh is refined sufficient (CFX, 2004)

Numerical setup

The computational grid was generated using the commercial mesh generator ICEM (ICEM, 2004). The main room was modelled using 120x100x59 nodes, and both the inlet and outlet were meshed using 40x30x59 nodes. The amount of nodes in this mesh, which is referred to as the medium mesh, was approximately 832,000. The first cell height was specified in order to ensure a y^+ value less than 1.7 everywhere, and the minimum angles were approximately 82 degrees. For the medium mesh, a sketch of the centre-plane of the room is shown in figure 5.

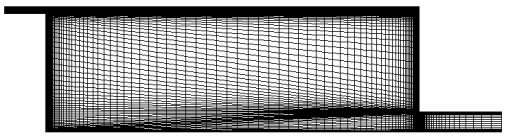

Figure 5: Computational mesh in the centre plane (z=1.5 m) of the room.

For the k-ε model a calculation using a coarse mesh of approximately 143,800 was carried out. The results obtained with the coarse mesh and the medium mesh showed only insignificant differences. Thus, it is reasonable to assume, that the presented results are not influenced by the grid size.

The discretised equations were solved using a coupled solver technology (CFX, 2004). Second order accuracy was employed using a blend factor of one. The convergence criterion was set to 0.00005. For the k-ε model, a solution converged to 0.0001 was compared to the solution converged to 0.00005. No significant differences existed between these two solutions, and the criterion of 0.00005 was therefore assumed to be sufficient for having a converged solution.

Numerical location of critical points

Finding the location of no-slip critical points in the centre plane is a straight forward matter when assuming the *w* component of the velocity is zero (Voigt *et al.*, 2003). Along the floor (y=0 *m*) the *u* component of velocity was monitored at *y*=0.001 *m*, and a critical point was depicted when a change in sign was found. Similar for the vertical wall below the inlet (*x*=0 *m*), the *v* component of velocity was monitored at *x*=0.001 *m*. A critical point was found when a change in sign occurs. The procedure for locating in-flow critical points was more complicated. A contour plot of the *u* velocity and *v* velocity was created, using only the contour with value zero. The location of the critical point was found at the intersection point between these two contours.

When classifying the critical points, several streamlines were drawn in the region surrounding the critical point. Based on the streamlines, it was a straightforward matter to determine if a no-slip critical point was an attachment point or a separation point. When classifying the in-flow critical points the procedure of using streamlines was more troublesome, since it could be difficult to distinguish between a centre and a spiral with a slow spiralling motion. To ensure that the used method does not predict a spiral point when the point is actually a centre, the method was tested for a pseudo 2-D calculation. For the pseudo 2-D calculation it was known that spiral points cannot occur. This can be ascribed to the Hamiltonian property of the stream function.

This concludes the presentation of the numerics, and the results are presented in the following section.

RESULTS

Pseudo 2-D simulation

The flow solver always solves the governing equations in three dimensions, and therefore a two dimensional flow was emulated using a slip wall boundary condition at the side walls (*z*=0 *m* and *z*=3 *m*) of the computational domain. The main reason for carrying out pseudo 2-D simulations was to ensure that the computational mesh did not introduce three dimensional effects in the flow. Moreover, the procedure for classifying critical points was verified.

The performance of turbulence models can be assessed by comparing velocities along two vertical lines at the central region in the centre plane of the room, *x*=3 *m* and *x*=6 *m* (Voigt, 2001). In figure 6 the numerical results using the k-ε model and the Menter model, respectively, are compared with measurements (Nielsen, 1990). For *x*=3 *m* it is observed that both models predict higher velocities in jet, 2.5 *m* < y < 3 *m*. For example at y= 2.9 *m*, the simulations gives a dimensionless velocity of approximately 0.83, while measurements gives a dimensional velocity of 0.78. At the floor, 0 *m* < y < 0.5 *m*, the k-ε model gives lower velocities, while the Menter model gives higher velocities than found in the LDA measurements (Nielsen, 1990). For example at y=0.1 *m* the k-ε model predicts a dimensionless velocity of -0.16, the measurements predicts a dimensionless velocity of -0.12, while the Menter model predicts a dimensionless velocity of -0.08. At x=6 *m*, both models show good agreement with measurements in the jet, while the Menter model predicts slightly lower velocities close to the floor. For example at y=0.01 *m* the Menter model gives a dimensionless velocity of -0.39 while measurements gives -0.32. In the core region, 0.5 *m* < y < 2.5 *m*, both models show a deviation from experiments which is difficult to explain. Despite the minor differences the overall conclusion is that both turbulence models provide results in good agreement with measurements. Thus, the tested turbulence models are concluded to be equally good for predicting mean velocities in the central part of the room.

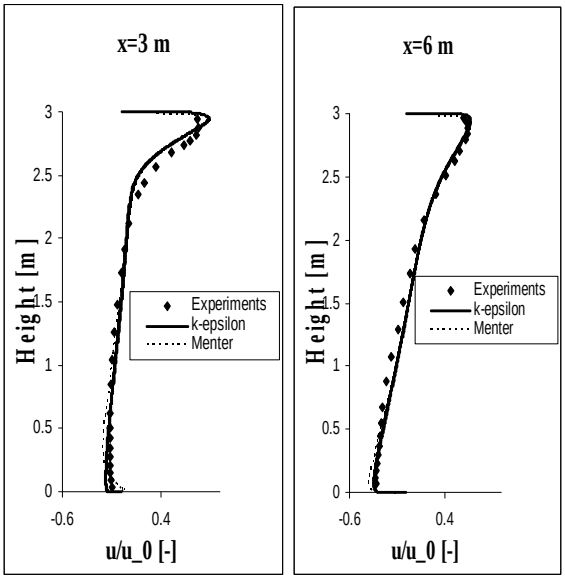

Figure 6: u component of velocity at two positions in the centre plane of the room. Experiments are LDA measurements (Nielsen, 1990)

Next the location and type of stagnation points are evaluated. Both models predicted a separation point on the floor and an attachment point on the wall. The k-ε model gives significant lower values than experiments, see table 1, while the Menter model leads to values which are larger than in experiments.

Table 1
Distance from origin to no-slip critical points. Experiments are based on PIV measurements (Pedersen & Meyer, 2002)

	k-ε	Menter	Experiments
Separation [*m*]	0.23	3.47	2.78
Attachment [*m*]	0.28	2.48	1.78

A similar trend is observed for the location of the in-flow critical point. The k-ε model predicts the centre point at (x,y) ≈ (0.11 *m*,0.09 *m*), while this is located at (x,y) ≈ (0.90 *m*,1.13 *m*) using the Menter model. In the measurements the in-flow critical point is an unstable spiral point, and it is located at (x,y) ≈ (0.51 *m*,0.72 *m*). The different location of the critical points leads to significant different flow pattern in the first third of the room. The k-ε model predicts a recirculation zone which is almost negligible in size, see figure 7, while the Menter model predicts a recirculation which covers almost one third of the room length.

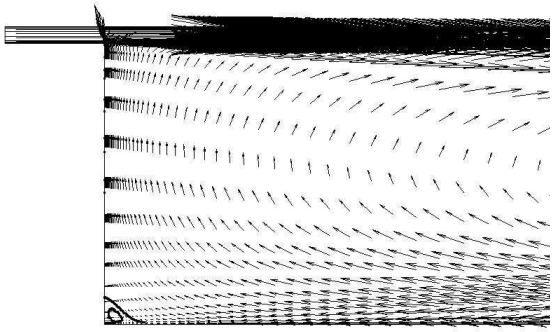

Figure 7: Streamlines in the centre plane of the room (z=1.5 m) based on pseudo 2-D simulations using the k-ε model. Only half of the room is displayed.

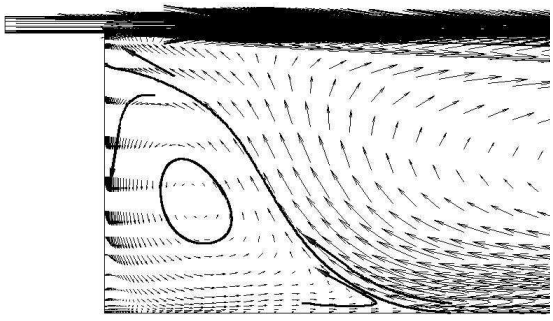

Figure 8: Streamlines in the centre plane of the room (z=1.5 m) based on pseudo 2-D simulations using the Menter model. Only half of the room is displayed.

From the streamlines in figure 7 and figure 8, the numerical in-flow critical point can be characterized as a centre, while the measurements predict a spiral point (Voigt, 2002). The flow pattern at a plane through y=0.5 *m* is shown in figure 9. From the streamlines it is obvious that the flow is parallel which implies, that the *w* velocity component is zero everywhere in the computational domain. Therefore, the flow must be two dimensional for *z* constant, which implies that only centres and saddles can exist. Based on figure 7 and figure 8, the topology for a pseudo 2-D simulation is shown in figure 10. Thus, it is concluded that a pseudo 2-D simulation could never capture the spiral point found in the measurements. Another important conclusion drawn from these simulations is that the numerical setup is sufficient for distinguishing between centres and spiral points.

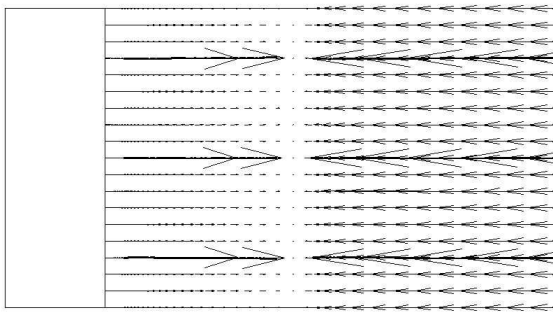

Figure 9: Streamline for y=0.5 m. The flow is seen to be parallel with respect to z.

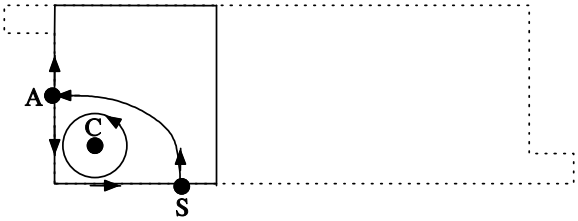

Figure 10: Flow topology related to recirculation zone below occurring below the inlet. The k-ε and the Menter model predicted the same topology.

This concludes the presentation of the pseudo 2-D simulations. It was concluded that the k-ε model and Menter model appeared to be equally good for predicting the mean quantities in the central part of the room. However, away from the central part of the room, the k-ε model was bad for predicting the size of the recirculation zone occurring below the inlet. Moreover, it was concluded that the present numerics are sufficient for classifying the critical points. Finally it was concluded that a pseudo 2-D simulation can never capture the flow pattern obtained in experiments, since the flow is parallel for all values of *z*.

3-D simulation

Using the same grid as for the pseudo 2-D simulations, the side walls of the computational domain were set to a no-slip wall. This introduces shear at the side walls, which leads to simulations in better agreement with the physical setup.

The performance of the turbulence models were assessed by the mean quantities in the central part of the room, see figure 11. The trends observed were similar to those found for the pseudo 2-D simulations, except in the core region 0.5 *m* < y < 2.5 *m* at x=3 *m*. In this region the k-ε model seems to be in better agreement with experiments than the Menter model. Despite this difference it is the author's opinion that the two models are equally good for predicting the mean velocities in the central part of the room.

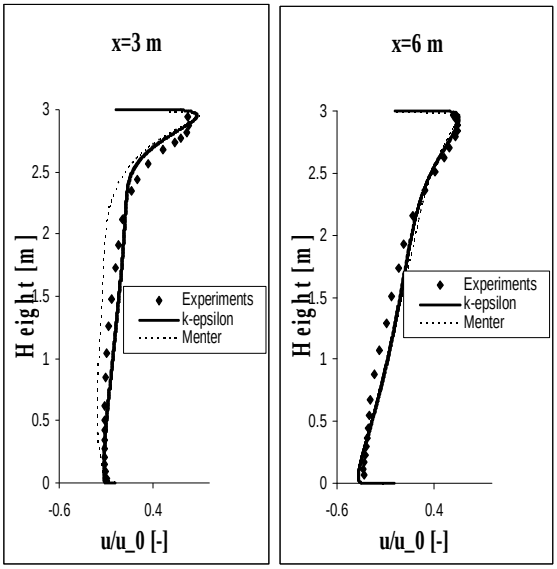

Figure 11: u component of velocity at two positions in the centre plane of the room. Experiments are LDA measurements (Nielsen, 1990)

Next, the location and type of critical points were evaluated. Both models predicted a separation point on the floor and an attachment point on the wall. The locations are summarised in table 2. By comparing the values in table 2 with the values in table 1, the no-slip walls seem to suppress the recirculation zone.

Table 2
Distance from origin to no-slip critical points. Experiments are based on PIV measurements (Pedersen & Meyer, 2002)

	k-ε	Menter	Experiments
Separation [m]	0.06	2.60	2.78
Attachment [m]	0.27	2.25	1.78

For the k-ε model the in-flow critical point is located at (x,y)≈ (0.06 *m*,0.003 *m*), while for the Menter model the in-flow critical point is located at (x,y)≈ (0.77 *m*,0.90 *m*). This should be compared to the experimentally found in-flow critical point at (x,y)≈ (0.51 *m*,0.72 *m*). As for the pseudo 2-D simulations, the two turbulence models predict significant different flow patterns when 3-D simulations are carried out. The results based on the 3-D simulations are shown in figure 12 and figure 13. The k-ε model predicts a recirculation zone which is almost negligible in size, while the Menter model predicts a recirculation which covers approximately one third of the room length. Comparing with measurements, figure 14, it is obvious that the Menter model is superior to the k-ε model.

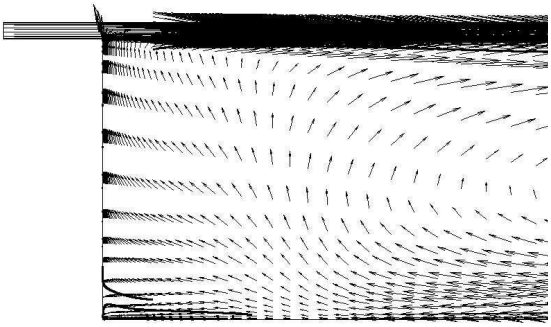

Figure 12: Streamlines in the centre plane of the room (z=1.5 m) based on 3-D simulations using the k-ε model. Only half of the room is displayed.

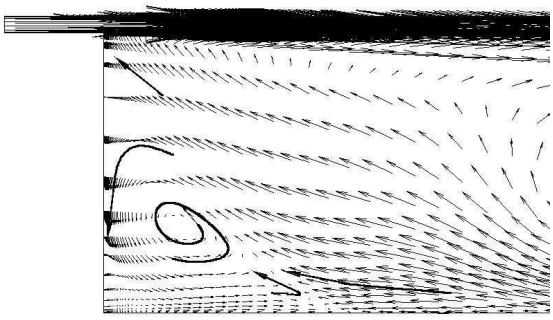

Figure 13: Streamlines in the centre plane of the room (z=1.5 m) based on 3-D simulations using the Menter model. Only half of the room is displayed.

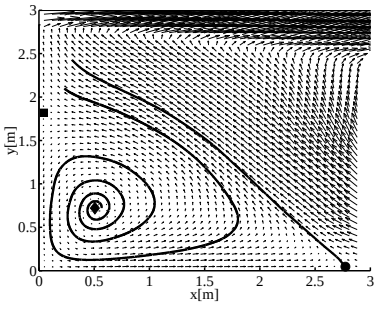

Figure 14: Streamlines in the centre plane of the room (z=1.5 m) based on experiments (Pedersen &Meyer, 2002).

From the streamlines in figure 12 it is not possible to classify the in-flow critical point for the simulation using the k-ε model, while the streamlines in figure 13 indicates that the Menter model predicts a stable spiral point. The critical point is concluded to be stable spiral point since the streamline shows a

spiralling motion towards the critical point. The direction of the spiralling motion is determined by the vectors near the streamline. In contrast, the measurements suggest an unstable spiral point, see figure 14. In the measurements the critical point is concluded to be an unstable spiral point since the streamline is spiralling away from the critical point. The direction of the spiralling motion is again determined by looking at the vectors near the streamline. In figure 15 the flow pattern in a plane, y=0.50 *m*, is shown. This indicates that the flow is highly three dimensional and the streamlines show how an unstable trajectory emanates from the spiral point into the flow. This explains why the in-flow critical point has changed from a centre in the pseudo 2-D simulations to a stable spiral point in the 3-D simulations. If an unstable trajectory emanates from the spiral point in the z direction, the spiral point cannot be unstable according to the theory from non linear differential equations (Grimshaw, 1990). Thus, the Menter model predicts a flow pattern in agreement with theory. Since no three dimensional flow topology is available from the measurements, it is not possible to draw further conclusions on the differences between experiments and simulations. The topology based on the Menter model and experiments is shown in figure 16.

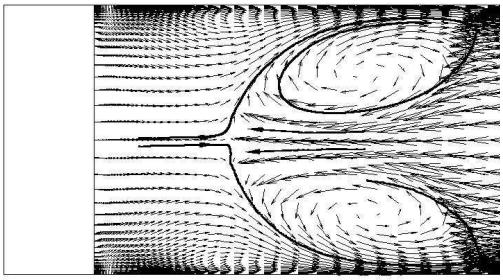

Figure 15: Streamline for y=0.50 m. The flow is seen to be symmetric around z=1.5 m.

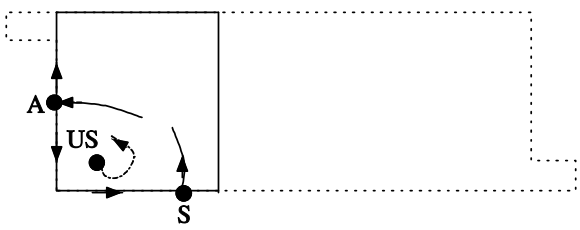

Figure 16: Flow topology related to the recirculation zone occurring below the inlet. The experiments predicted an unstable in-flow spiral point, while the Menter model predicted a stable in-flow spiral point.

This concludes the presentation of the 3-D simulations. It was concluded, that employing the no slip wall boundary condition at the side walls tends to suppress the recirculation zone below the inlet. When predicting mean quantities in the central region of the room, the turbulence models were almost equally good. However, away from the central part of the room, the k-ε model was bad for predicting the size of the recirculation zone occurring below the inlet. Experiments and the Menter model predicted a different topology for the in-flow critical point, but since experiments were only available in the centre plane, it was not possible to explain this difference. However, the Menter model predicted a topology in agreement with theory, and therefore it is reasonable to believe, that the differences are caused by experimental uncertainties.

CONCLUSION

In the present work a topological approach was used to evaluate two turbulence models for simulating the flow in an enclosure. In particular the location and classification of critical points was examined. Moreover topology was used to explain the differences between pseudo 2-D simulations, 3-D simulations and experiments. Pseudo 2-D simulations using slip boundary conditions at the side walls were carried out to justify, that the used numerical setup were sufficient for classifying critical points. When assessing the numerical setup the topological apparatus turned out to be a valuable tool, since this provides theoretical information about the possible flow patterns. Three dimensional effects are introduced when the boundary conditions at the side walls are changed to a no-slip condition. Based on the full 3-D simulations the following important conclusions were drawn:

- The k-ε model and the Menter model performed equally good when mean velocities in the central region of the room were predicted
- The k-ε model was bad for predicting the size of the recirculation zone below the inlet, while the Menter model was much better.
- The Menter model and experiments predicted a different topology for the inflow critical point below the inlet. Since experiments are only available in the centre plane it is not possible to conclude further on this difference. However, based on theory from non-linear differential equations the topology predicted by the Menter model is consistent with the three dimensional flow structures.
- The topological apparatus has turned out to be a valuable tool for assessing the accuracy of numerical techniques and for explaining similarities and differences between experiments and simulations.

In general it is suggested that a Menter type of model should be used for HVAC applications of this kind.

NOMENCLATURE

LATIN

$C_{\varepsilon 1}$, $C_{\varepsilon 2}$, C_{μ}: Empirical constants in the k-ε model
f_1, f_2: Damping functions in the k-ε model
F_1: Blending function
h: Height of inlet
k: Turbulent kinetic energy
L: Length of room
L_i: Length of inlet
L_o: Length of outlet
P_k: Turbulence production
t: time or Height of outlet
U_i: Mean velocity components in turbulence transport equations
u_0: Inlet velocity
u, v, w: Velocity components in x,y,z direction
W: Width of room
x_i: Spatial directions in turbulence transport equations

GREEK

α_3,: Constant in the BSL k-ω model of Menter
β_3, β': Constant in the BSL k-ω model of Menter
ε: Dissipation of turbulent kinetic energy
ω: Specific dissipation rate
ρ: Density
μ: Dynamic viscosity
μ_t: Eddy viscosity
σ_k, σ_ε: Constants in the k-ε model
σ_{k3},$\sigma_{\omega 2}$, $\sigma_{\omega 3}$: Constants in the BSL k-ω model of Menter

REFERENCES

CFX Solver Manual, 2004, Ansys INC.

Davidson, L., Nielsen, P.V. & Topp, C. 2000. Low-Reynolds Number Effects in Ventilated Rooms: a Numerical Study", ROOMVENT 2000, vol. 1, 307-312.

Grimshaw, D., 1990. Nonlinear Ordinary Differential Equations, Blackwell Scientific Publications, 276-314.

ICEM User Manual, 2004, Ansys INC.

Nielsen, P.V., 1990. Specification of a Two dimensional Testcase, IEA Annex 20 Research Item 1.45, Technical Report, University of AAlborg, Denmark.

Hartnack, J.N., 1999. Streamline Topologies near a Fixed Wall using Normal Forms, Acta Mechanica, vol. 136, issue 1, 55-75.

Menter, F.R. 1994. Two-equation Eddy-Viscosity Turbulence Models for Engineering Applications", AIAA Journal, Vol. 32, No. 8, August, 1598-1605.

Pedersen, J.M. & Meyer, K.E., 2002. POD Analysis of Flow Structures in a Scale Model of a Ventilated Room, Experiments in Fluids 33, 940-949.

Sørensen, D.N. & Nielsen, P.V., 2003. Quality control of computational fluid dynamics in indoor environments. Indoor Air, 13, 2-17.

Voigt, L.K., 2001, Navier-Stokes Simulation of Airflow in Rooms and Around a Human Body Ph.D. Thesis, Department of Mechanical Engineering, Fluid Mechanics Section, DTU.

Voigt, L.K., 2002. Validation of Turbulence Models using Topological Aspects, ROOMVENT 2002, 173-176

Voigt, L.K., Sørensen, J.N., Pedersen, J.M. & Brøns, M. 2003. Review of four turbulence models using topology, In proceedings of the 8th International IBPSA Conference, Eindhoven, Netherlands, August 11-14, 2003, pp. 1325-1331.